Robust H-inf Output Feedback Trajectory Tracking Control

for Steer-by-Wire Four-Wheel Independent Actuated Electric Vehicles

Course: Robust Control System

By

TOUHA KHALID

MUHAMMAD NAWAZ AWAN

Submitted to the faculty of Engineering at PIEAS in partial fulfillment of requirements for the Degree of MS Systems Engineering

Department of EE

Pakistan Institute of Engineering & Applied Sciences,

Nilore, Islamabad, Pakistan.

Table of Contents

Abstract 1

1. Introduction 2

2. Literature Review 3

2.1 AFS, DYC, and Integrated Vehicle Stability Control **3**

2.2 Trajectory Tracking Control under Uncertainty **3**

2.3 Robust $H\infty$ Control and Output Feedback **4**

2.4 Steer-by-Wire Dynamics in Control Design **4**

2.5 Positioning of This Work **4**

3. System Modeling and Problem Formulation 5

Notation / geometry (as on the figure) **5**

3.1 Trajectory Tracking Error Dynamics **6**

3.2 Vehicle Planar Dynamics **7**

3.3 Tire and Wheel Dynamics **7**

3.4 Steer-by-Wire Actuator Dynamics **8**

3.5 LPV Modeling with Parametric Uncertainty **8**

3.6 Control-Oriented Model and Problem Statement **9**

4. Robust $H\infty$ Output-Feedback Controller Design 9

4.1 Motivation for Dynamic Output-Feedback Control **10**

4.2 Dynamic Output-Feedback Controller Structure **10**

4.3 Closed-Loop System Representation **10**

4.4 Robust $H\infty$ Performance Objective **11**

4.5 Actuator Constraint Formulation **11**

4.6 LMI-Based Robust $H\infty$ Synthesis **11**

Prove of Theorem 1: 12

Prove of Theorem 2: 15

4.7 Controller Parameter Recovery **17**

5. Implementation and Numerical Challenges 18

5.1 Implementation Environment and Tools **18**

5.2 Numerical Instability in Standard Controller Reconstruction **18**

5.3 Direct LMI-Based Controller Design with Regularization **19**

5.4 Physical Consistency and Feedback Direction Correction **19**
5.5 Performance Tuning and Feasibility Trade-Off **19**
5.6 Final Controller Implementation **20**
6. Simulation Results and Robustness Extension 20
6.1 Nominal Closed-Loop Performance **21**
Lateral Tracking Performance 21
Yaw Stability 21
Control Effort and Actuator Constraints 22
Controller Gain Validation 22
6.2 Robustness Extension: Parameter Variation Analysis **22**
Test Scenarios 22
Quantitative Performance Comparison 23
Discussion of Robustness Results 23
6.3 Summary of Simulation Findings **24**
7. Discussion 24
7.1 Robustness Versus Performance Trade-Off **24**
7.2 Numerical Conditioning and Practical Implementability **25**
7.3 Importance of Physics-Informed Design **25**
7.4 Actuator Constraints and Energy Usage **25**
7.5 Implications for Autonomous Vehicle Control **25**
7.6 Summary of Key Insights **26**
7. Conclusions 26
Code and Data Availability 27

List of Figures

Figure 1: Trajectory Tracking process in FWIA EV 6
Figure 2: Closed-loop response under nominal operating conditions.....21
Figure 3: Extension (Parameter Variation Analysis).....23

List of Tables

Table 1: Comparison 23

Abstract

This report presents the reproduction, implementation, and extension of a robust H_∞ dynamic output-feedback trajectory tracking controller for steer-by-wire four-wheel independent actuated (4WIA) electric vehicles. A polytopic linear parameter-varying (LPV) model is employed to capture time-varying longitudinal velocity and bounded parametric uncertainties arising from variations in vehicle mass, tire cornering stiffness, and road adhesion. To address the limited availability of measurable states, a dynamic output-feedback control strategy is adopted, eliminating the need for sideslip angle measurement.

The controller is synthesized using linear matrix inequalities (LMIs) to guarantee robust asymptotic stability, H_∞ disturbance attenuation, and actuator constraint satisfaction. Practical implementation challenges, including numerical instability and physically inconsistent feedback behavior, are addressed through direct LMI-based controller synthesis, regularization to limit gain magnitudes, and physics-informed correction of control gain signs.

Simulation results demonstrate fast and accurate trajectory tracking, stable yaw dynamics, and strict adherence to actuator limits under nominal conditions. A robustness extension is performed by evaluating the controller under significant vehicle mass increase and severe reduction in road adhesion. The results show that the closed-loop system remains stable and exhibits graceful performance degradation under adverse conditions, confirming the robustness of the proposed control strategy. This study not only reproduces the results of the reference work but also provides practical insights into the implementation and validation of robust control methods for autonomous electric vehicles.

1. Introduction

Four-wheel independent actuated (4WIA) electric vehicles have emerged as a promising platform for advanced vehicle dynamics control due to their high actuation redundancy and flexibility. By independently controlling the driving torque of each wheel, 4WIA electric vehicles can generate a direct yaw moment without relying solely on steering inputs, thereby significantly enhancing vehicle stability, maneuverability, and safety. When combined with steer-by-wire technology, which eliminates the mechanical linkage between the steering wheel and the front wheels, such vehicles provide a highly suitable architecture for autonomous and intelligent driving applications.

A fundamental requirement for autonomous driving systems is **accurate and robust trajectory tracking**, which ensures that the vehicle follows a desired path while maintaining stability and passenger comfort. However, trajectory tracking control for steer-by-wire 4WIA electric vehicles is particularly challenging due to several practical issues. These include parametric uncertainties arising from variations in vehicle mass, tire cornering stiffness, and road adhesion conditions, as well as time-varying longitudinal velocity during real driving scenarios. In addition, certain vehicle states, most notably the sideslip angle, are difficult to measure accurately using low-cost sensors, which limits the applicability of conventional state-feedback control strategies.

To address robustness against uncertainties and external disturbances, H_∞ **control theory** has been widely adopted in vehicle dynamics and trajectory tracking problems. In particular, linear parameter-varying (LPV) modeling combined with linear matrix inequality (LMI)–based synthesis provides a systematic framework for handling time-varying parameters and bounded uncertainties. Several studies have investigated integrated control strategies combining active front steering (AFS) and direct yaw moment control (DYC) using robust or gain-scheduled controllers. These approaches have demonstrated improved handling performance and yaw stability under uncertain operating conditions. However, many existing works neglect the **dynamic characteristics of the steer-by-wire actuator**, or assume full-state availability, which limits their practical applicability.

Recently, Li *et al.* proposed a **robust H_∞ dynamic output-feedback trajectory tracking control strategy** for steer-by-wire 4WIA electric vehicles based on a polytopic LPV model. Their approach explicitly incorporates the dynamics of the steer-by-wire system, accounts for time-varying longitudinal velocity, and considers multiple sources of parametric uncertainty. By employing dynamic output feedback, the controller avoids reliance on sideslip angle measurements while guaranteeing robust stability, disturbance attenuation, and actuator constraint satisfaction through LMI-based synthesis.

The objective of this project is to **reproduce, validate, and extend** the results presented in the aforementioned work. Specifically, the main contributions of this project are threefold. First, the complete LPV-based trajectory tracking model and robust H_∞ output-feedback controller is reconstructed and implemented in MATLAB using YALMIP and an SDP solver. Second, the reproduced controller is rigorously validated through time-domain

simulations, with particular attention paid to numerical stability, physical consistency of control actions, and closed-loop performance. Third, an extension is carried out in the form of a robustness stress test, where the designed controller is evaluated under significant variations in vehicle mass and road adhesion conditions to assess conservatism and robustness margins beyond those reported in the original paper.

Unlike a purely theoretical reproduction, this project emphasizes **engineering realism**, documenting key numerical and physical challenges encountered during implementation and the corrective measures taken to ensure stable and meaningful control behavior. As such, the report not only verifies the results of the original study but also provides practical insights into robust controller synthesis for over-actuated electric vehicles.

To support reproducibility, all implementation files and detailed derivations developed in this project are made publicly available in an online GitHub repository.

2. Literature Review

Trajectory tracking control for autonomous and electric vehicles has received significant research attention due to its direct impact on vehicle safety, stability, and ride comfort. For four-wheel independently actuated (FWIA) electric vehicles equipped with steer-by-wire systems, the problem becomes more challenging because of over-actuation, parameter uncertainty, actuator dynamics, and limited state measurement availability.

2.1 AFS, DYC, and Integrated Vehicle Stability Control

Active Front Steering (AFS) and Direct Yaw Moment Control (DYC) are two widely studied techniques for improving vehicle lateral stability and handling performance. AFS enhances maneuverability and driving comfort by modifying steering input, whereas DYC exploits differential wheel torques to generate corrective yaw moments. However, relying on either AFS or DYC alone has inherent limitations, particularly when tires operate in nonlinear regions or under low-friction conditions.

To overcome these limitations, integrated AFS/DYC control architectures have been proposed to improve stability, safety, and maneuverability simultaneously. Prior studies demonstrate that such integrated control schemes outperform single-actuator approaches, especially for FWIA electric vehicles where yaw moments can be generated rapidly and precisely through in-wheel motors

2.2 Trajectory Tracking Control under Uncertainty

Beyond stability control, accurate trajectory tracking is a core requirement for autonomous driving. Numerous control strategies have been proposed to address trajectory tracking in the presence of model uncertainty, time-varying vehicle speed, and external disturbances.

These include adaptive control, sliding mode control, model predictive control (MPC), and gain-scheduled control approaches.

Among these, Linear Parameter-Varying (LPV) modeling has emerged as a powerful framework for handling time-varying longitudinal velocity and uncertain vehicle parameters. By expressing the vehicle dynamics as a convex combination of multiple linear models, LPV techniques enable systematic controller synthesis with guaranteed robustness properties. Robust LPV-based control has been successfully applied to FWIA electric vehicles for lateral motion control and path following under varying operating conditions

2.3 Robust H_∞ Control and Output Feedback

Robust H_∞ control is widely recognized as an effective method for handling structured uncertainties and external disturbances. When combined with LPV modeling, H_∞ control provides strong guarantees of robust stability and disturbance attenuation across the entire operating envelope.

However, most robust control formulations assume full-state feedback, which is impractical for real vehicles because certain states—most notably the sideslip angle—are difficult to measure accurately using low-cost sensors. To address this limitation, dynamic output-feedback control strategies have been proposed, allowing robust controller synthesis using only measurable outputs.

Previous studies have demonstrated the effectiveness of robust H_∞ dynamic output-feedback controllers for FWIA electric vehicles, particularly in integrated AFS/DYC frameworks that do not rely on sideslip angle measurement

2.4 Steer-by-Wire Dynamics in Control Design

While many existing works focus on lateral vehicle dynamics, fewer studies explicitly incorporate the **dynamic characteristics of the steer-by-wire actuator** into the control-oriented model. Neglecting steering actuator dynamics can lead to degraded tracking performance, increased control effort, and reduced ride comfort.

Recent research highlights that including steer-by-wire dynamics in the control design yields improved tracking accuracy and smoother control actions, particularly during aggressive maneuvers such as lane changes. Nevertheless, incorporating actuator dynamics increases model complexity and exacerbates numerical challenges in robust controller synthesis.

2.5 Positioning of This Work

Motivated by the above observations, the reference study proposes a robust H_∞ dynamic output-feedback trajectory tracking controller for steer-by-wire FWIA electric vehicles using a polytopic LPV framework. The design explicitly accounts for:

- time-varying longitudinal velocity,
- parameter uncertainty in mass, inertia, tire stiffness, and road adhesion,
- steer-by-wire actuator dynamics,
- actuator saturation constraints,
- and the absence of sideslip angle measurement

This project reproduces the core control framework of that work using MATLAB-based simulation and further extends it through:

1. detailed numerical implementation and debugging of the LMI-based synthesis,
2. physics-informed corrections to ensure practical realizability,
3. robustness evaluation under explicit mass and friction variation scenarios.

As a result, this study not only validates the original methodology but also provides additional insight into the practical challenges and robustness characteristics of H_∞ output-feedback control for FWIA electric vehicles.

3. System Modeling and Problem Formulation

This section presents the dynamic modeling of the steer-by-wire four-wheel independent actuated (4WIA) electric vehicle and formulates the trajectory tracking control problem. The model explicitly accounts for the dynamic characteristics of the steer-by-wire system, time-varying longitudinal velocity, parametric uncertainty, and external disturbances. These features are essential for realistic trajectory tracking control in autonomous driving scenarios.

Notation / geometry (as on the figure)

- e_d: lateral deviation (distance from vehicle CG to nearest point T on desired path).
- $e_\varphi = \varphi_d - \varphi$: yaw angle error (desired yaw minus actual yaw).
- β: sideslip angle at CG (small).
- γ: yaw rate (paper's sign convention — see remark below).
- v_x: longitudinal velocity (assumed positive and large compared to lateral components).
- $\rho_T(\sigma)$: curvature of the desired trajectory at point T.

- F_{yf}, F_{yr}: front/rear lateral tire forces.
- C_f, C_r: cornering stiffnesses (front, rear).
- α_f, α_r: slip angles (front, rear).
- m: vehicle mass, I_z: yaw moment of inertia, l_f, l_r: distances from CG to front/rear axle.
- ΔM_z: direct yaw moment produced by differences in longitudinal wheel forces (actuation by hub motors).
- $I_w, w_i, T_i, F_{xi}, R_t, l_s$ — wheel inertia, wheel rotational speed, hub torque, longitudinal contact force, rolling radius, track-width related length, respectively.

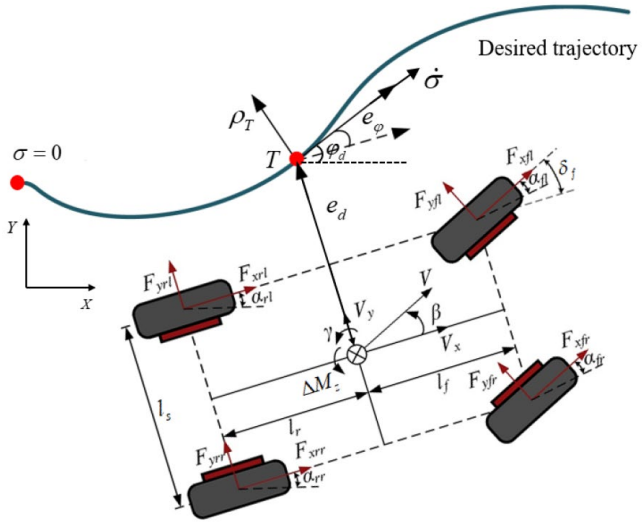

Figure 1: Trajectory Tracking process in FWIA EV

3.1 Trajectory Tracking Error Dynamics

Consider a 4WIA electric vehicle following a predefined planar reference trajectory. Let e_d denote the lateral deviation between the vehicle center of gravity (CG) and the closest point on the desired path, and let e_ϕ denote the yaw-angle error between the desired yaw angle and the actual vehicle yaw angle. The sideslip angle at the CG is denoted by β, and γ represents the vehicle yaw rate. The longitudinal velocity v_x is assumed to be positive and significantly larger than lateral velocity components.

Under small-angle assumptions commonly adopted in vehicle dynamics, the kinematic error dynamics of trajectory tracking can be expressed as

$$\begin{aligned} \dot{e}_d &= v_x e_\phi + v_x \beta + d_1, \\ \dot{e}_\phi &= \gamma + d_2, \end{aligned}$$

where d_1 and d_2 represent modeling errors and external disturbances, including the effect of path curvature. These equations describe how lateral and heading errors evolve as functions of vehicle motion states and disturbances.

3.2 Vehicle Planar Dynamics

Neglecting pitch and roll motions, the planar lateral and yaw dynamics of the vehicle are modeled using a standard bicycle-model representation. The lateral motion is described by the sideslip angle dynamics, while the yaw motion is governed by the yaw-rate dynamics. The equations of motion are given by

$$\begin{aligned} \dot{\beta} &= \frac{1}{m v_x}\left(F_{yf} + F_{yr}\right) + d_3, \\ \dot{\gamma} &= \frac{1}{I_z}\left(l_f F_{yf} - l_r F_{yr}\right) + \frac{1}{I_z}\Delta M_z + d_4, \end{aligned}$$

where F_{yf} and F_{yr} are the lateral tire forces at the front and rear axles, respectively. The parameters m and I_z denote the vehicle mass and yaw moment of inertia, while l_f and l_r are the distances from the CG to the front and rear axles. The term ΔM_z represents the direct yaw moment generated by differential wheel torques, and d_3 and d_4 capture unmodeled dynamics and external disturbances.

The direct yaw moment is produced by unequal longitudinal forces at the wheels and is expressed as

$$\Delta M_z = \sum_{i=1}^{4} (-1)^i F_{x_i} \frac{l_s}{2},$$

where F_{x_i} is the longitudinal force at the i-th wheel and l_s is the vehicle track width.

3.3 Tire and Wheel Dynamics

The rotational dynamics of each wheel are described by

$$I_w \dot{\omega}_i = T_i - F_{x_i} R_t,$$

where I_w is the wheel rotational inertia, ω_i is the wheel angular speed, T_i is the hub motor torque, and R_t is the tire rolling radius.

For small slip angles, the lateral tire forces are approximated using a linear tire model:

$$F_{yf} = \mu C_f \alpha_f, \qquad F_{yr} = \mu C_r \alpha_r,$$

where μ is the road adhesion coefficient, C_f and C_r are the cornering stiffnesses of the front and rear tires, and α_f and α_r are the front and rear slip angles.

The slip angles are geometrically related to vehicle motion by

$$\alpha_f = \beta + \frac{l_f}{v_x}\gamma - \delta_f, \qquad \alpha_r = \beta - \frac{l_r}{v_x}\gamma,$$

where δ_f denotes the front-wheel steering angle.

3.4 Steer-by-Wire Actuator Dynamics

Unlike conventional lateral control models, the dynamic behavior of the steer-by-wire actuator is explicitly incorporated. The steering subsystem is modeled as a second-order rotational system subject to motor torque, viscous damping, and tire-induced moments. The steering dynamics are given by

$$\ddot{\delta}_f = -\frac{\mu C_f (l_p + l_m)}{J_w}\beta - \frac{\mu C_f l_f (l_p + l_m)}{J_w v_x}\gamma + \frac{\mu C_f (l_p + l_m)}{J_w}\delta_f - \frac{b_w}{J_w}\dot{\delta}_f + \frac{\eta_m r_s k_m}{J_w} i_m + d_5,$$

where J_w and b_w are the steering system inertia and damping coefficient, respectively. The parameters l_p and l_m represent the aerodynamic and mechanical offsets of the steering system, η_m is the motor efficiency, r_s is the steering ratio, k_m is the motor constant, and i_m is the steering motor current. The disturbance term d_5 accounts for unmodeled effects and actuator uncertainties.

3.5 LPV Modeling with Parametric Uncertainty

In practical driving conditions, several vehicle parameters are subject to uncertainty, including the road adhesion coefficient, tire cornering stiffnesses, vehicle mass, and yaw moment of inertia. These parameters are modeled as nominal values plus bounded time-varying perturbations. Furthermore, the longitudinal velocity v_x is treated as a time-varying scheduling parameter.

To capture these effects, the system is formulated as a linear parameter-varying (LPV) model with scheduling vector

$$\rho = \begin{bmatrix} v_x & \frac{1}{v_x} & \frac{1}{v_x^2} \end{bmatrix}^T,$$

whose components vary within known bounds. By evaluating the LPV model at the vertices of the scheduling parameter domain, the system can be represented as a polytopic model with eight vertices:

$$\dot{x}(t) = \sum_{i=1}^{8} \alpha_i(\rho, t)\left[(A_{ni} + \Delta A_i)x(t) + (B_{ni} + \Delta B_i)u(t) + \bar{d}(t)\right],$$

where $\alpha_i(\rho, t)$ are barycentric weights satisfying $\sum_{i=1}^{8} \alpha_i = 1$. The matrices A_{ni} and B_{ni} represent the nominal system matrices at each vertex, while ΔA_i and ΔB_i capture norm-bounded uncertainties. The lumped disturbance vector $\bar{d}(t)$ aggregates modeling errors and external disturbances.

3.6 Control-Oriented Model and Problem Statement

Define the state vector as

$$x = \begin{bmatrix} e_d & e_\phi & \beta & \gamma & \delta_f & \dot{\delta}_f \end{bmatrix}^T,$$

and the control input vector as

$$u = [\Delta M_z \quad i_m]^T.$$

While the lateral deviation, yaw error, yaw rate, steering angle, and steering rate are measurable using onboard sensors, the sideslip angle is difficult to obtain accurately with low-cost sensing hardware. Consequently, a state-feedback controller is impractical. Instead, the measured output is selected as

$$y = C_1 x,$$

which excludes the sideslip angle, while the performance output is defined as

$$z = C_2 x,$$

where all states are included to evaluate tracking performance.

The control objective is to design a **robust H_∞ dynamic output-feedback controller** such that the closed-loop system:

1. is robustly asymptotically stable under parameter uncertainty and disturbances,
2. satisfies a prescribed H_∞ disturbance attenuation level,
3. respects actuator constraints on steering motor current and yaw-moment generation.

This formulation provides the foundation for the robust controller synthesis developed in the next section.

4. Robust H_∞ Output-Feedback Controller Design

This section presents the robust H_∞ dynamic output-feedback controller design for the steer-by-wire 4WIA electric vehicle based on the polytopic LPV model derived in Section 2. The controller is designed to ensure robust stability, disturbance attenuation, and actuator safety under parameter uncertainty and time-varying longitudinal velocity, without requiring measurement of the vehicle sideslip angle.

4.1 Motivation for Dynamic Output-Feedback Control

For the trajectory tracking control problem formulated in Section 2, full state feedback would require accurate measurement of all vehicle states, including the sideslip angle β. However, β is difficult to measure reliably using low-cost onboard sensors and is highly sensitive to noise and parameter variation. Consequently, a full state-feedback controller is impractical for real-world implementation.

Static output-feedback control, while simpler, is generally too restrictive for robust H_∞ synthesis in uncertain LPV systems and often leads to infeasible LMIs. Therefore, a **dynamic output-feedback (DOF) controller** is adopted. By introducing controller internal states, dynamic output-feedback provides sufficient degrees of freedom to satisfy robust stability, performance, and actuator constraints simultaneously.

4.2 Dynamic Output-Feedback Controller Structure

The robust dynamic output-feedback controller is designed in a gain-scheduled form consistent with the polytopic LPV representation of the plant. The controller is defined as

$$\begin{aligned} \dot{x}_c(t) &= \sum_{i=1}^{8}\sum_{j=1}^{8} \alpha_i(\rho,t)\alpha_j(\rho,t)A_{cij}x_c(t) + \sum_{j=1}^{8} \alpha_j(\rho,t)B_{cj}y(t), \\ u(t) &= \sum_{j=1}^{8} \alpha_j(\rho,t)C_{cj}x_c(t) + D_c y(t), \end{aligned}$$

where $x_c(t)$ denotes the controller state vector, and A_{cij}, B_{cj}, C_{cj}, and D_c are controller gain matrices to be determined via LMI-based synthesis. The scheduling parameters $\alpha_i(\rho,t)$ are the barycentric coordinates of the polytopic LPV model.

This controller structure allows the control gains to vary smoothly with the scheduling parameters while maintaining convexity of the synthesis conditions.

4.3 Closed-Loop System Representation

Define the augmented state vector

$$\bar{x}(t) = \begin{bmatrix} x(t) \\ x_c(t) \end{bmatrix}.$$

By combining the plant dynamics and the controller dynamics, the closed-loop system can be expressed in the following polytopic form:

$$\begin{aligned} \dot{\bar{x}}(t) &= \sum_{i=1}^{8}\sum_{j=1}^{8} \alpha_i(\rho,t)\alpha_j(\rho,t)\left[\left(\bar{A}_{ij} + \bar{H}\Lambda\bar{L}_{ij}\right)\bar{x}(t) + \bar{B}\bar{d}(t)\right], \\ z(t) &= \bar{C}\bar{x}(t), \end{aligned}$$

where $\bar{A}_{ij}$ represents the nominal closed-loop system matrices at each vertex, $\bar{H}\Lambda\bar{L}_{ij}$ captures the structured norm-bounded uncertainty, and $\bar{d}(t)$ denotes the lumped disturbance vector.

This formulation explicitly incorporates:

- LPV scheduling via convex combinations,
- structured parametric uncertainty,
- and dynamic output-feedback control.

4.4 Robust H_∞ Performance Objective

The control objective is to ensure that the closed-loop system is robustly asymptotically stable and satisfies the H_∞ disturbance attenuation condition

$$\int_0^t z^T(\tau)z(\tau)\,d\tau \le \gamma^2 \int_0^t \bar{d}^T(\tau)\bar{d}(\tau)\,d\tau,$$

for all admissible uncertainties and disturbances, where $\gamma > 0$ is the prescribed attenuation level.

This inequality ensures that the energy of the tracking error remains bounded relative to the energy of external disturbances, providing robustness against modeling errors, parameter variation, and unmodeled dynamics.

4.5 Actuator Constraint Formulation

In addition to stability and performance, the controller must respect physical actuator limits. The control inputs consist of the steering motor current and the direct yaw moment command, which must satisfy

$$|u_s(t)| \le u_s^{\max}, \quad s = 1,2,$$

where $u_s^{\max}$ denotes the maximum allowable magnitude of each control input.

These constraints are incorporated directly into the controller synthesis via additional LMIs, ensuring that the resulting controller is not only robust but also physically realizable.

4.6 LMI-Based Robust H_∞ Synthesis

To derive tractable synthesis conditions, a quadratic Lyapunov function candidate is selected as

$$V(\bar{x}) = \bar{x}^T P \bar{x},$$

where P is a symmetric positive-definite matrix. By applying Lyapunov stability theory, Schur complements, and an S-procedure-based uncertainty elimination technique, sufficient LMI conditions are obtained that guarantee:

1. robust asymptotic stability of the closed-loop system,
2. satisfaction of the H_∞ performance inequality,
3. enforcement of actuator constraints.

These conditions are formulated as a finite set of LMIs evaluated at each vertex of the polytopic model. The resulting synthesis problem is convex and can be efficiently solved using semidefinite programming.

Theorem 1 provides sufficient LMI conditions ensuring robust stability and H_∞ performance, while **Theorem 2** introduces a change of variables that converts the nonlinear matrix inequalities into solvable linear matrix inequalities.

Prove of Theorem 1:

The Setup: System and Stability

We start with the augmented closed-loop system dynamics

$$\dot{\bar{x}}(t) = \left(\bar{A}_{ij} + \Delta\bar{A}_{ij}\right)\bar{x}(t) + \bar{B}\bar{d}(t)$$

$$z(t) = \bar{C}\bar{x}(t)$$

We use the Lyapunov function:

$$V(\bar{x}) = \bar{x}^T P \bar{x}$$

We aim to satisfy the H_∞ performance criterion:

$$\dot{V} + z^T z - \omega^2 \bar{d}^T \bar{d} < 0$$

2. Expanding the Time Derivative ($\dot{V}$)

First, calculate the time derivative of the Lyapunov function along the system trajectories.

$$\dot{V} = \dot{\bar{x}}^T P \bar{x} + \bar{x}^T P \dot{\bar{x}}$$

Substitute $\dot{\bar{x}} = \left(\bar{A}_{ij} + \Delta\bar{A}_{ij}\right)\bar{x} + \bar{B}\bar{d}$ into the equation:

$$\dot{V} = \left[\left(\bar{A}_{ij} + \Delta\bar{A}_{ij}\right)\bar{x} + \bar{B}\bar{d}\right]^T P\bar{x} + \bar{x}^T P\left[\left(\bar{A}_{ij} + \Delta\bar{A}_{ij}\right)\bar{x} + \bar{B}\bar{d}\right]$$

Expand the transpose terms (using $(AB)^T = B^T A^T$):

$$\dot{V} = \left(\bar{x}^T\left(\bar{A}_{ij} + \Delta\bar{A}_{ij}\right)^T + \bar{d}^T\bar{B}^T\right)P\bar{x} + \bar{x}^T P\left(\bar{A}_{ij} + \Delta\bar{A}_{ij}\right)\bar{x} + \bar{x}^T P\bar{B}\bar{d}$$

Distribute the multiplication:

$$\dot{V} = \bar{x}^T\left(\bar{A}_{ij} + \Delta\bar{A}_{ij}\right)^T P\bar{x} + \bar{d}^T\bar{B}^T P\bar{x} + \bar{x}^T P\left(\bar{A}_{ij} + \Delta\bar{A}_{ij}\right)\bar{x} + \bar{x}^T P\bar{B}\bar{d}$$

Combine the scalar cross terms (since $\bar{d}^T\bar{B}^T P\bar{x} = \left(\bar{x}^T P\bar{B}\bar{d}\right)^T$ and the result is a scalar, they are equal):

$$\dot{V} = \bar{x}^T\left(\left(\bar{A}_{ij} + \Delta\bar{A}_{ij}\right)^T P + P\left(\bar{A}_{ij} + \Delta\bar{A}_{ij}\right)\right)\bar{x} + 2\bar{x}^T P\bar{B}\bar{d}$$

3. Formulating the Matrix Inequality

Substitute the expanded $\dot{V}$ and $z = \bar{C}\bar{x}$ into the H_∞ condition $\dot{V} + z^T z - \omega^2\bar{d}^T\bar{d} < 0$:

$$\bar{x}^T\left(\left(\bar{A}_{ij} + \Delta\bar{A}_{ij}\right)^T P + P\left(\bar{A}_{ij} + \Delta\bar{A}_{ij}\right)\right)\bar{x} + 2\bar{x}^T P\bar{B}\bar{d} + \bar{x}^T\bar{C}^T\bar{C}\bar{x} - \bar{d}^T\omega^2 I\bar{d} < 0$$

Group the terms into a block matrix multiplied by the vector $\begin{bmatrix}\bar{x}\\ \bar{d}\end{bmatrix}$:

$$\begin{bmatrix}\bar{x}\\ \bar{d}\end{bmatrix}^T\begin{bmatrix}\left(\bar{A}_{ij} + \Delta\bar{A}_{ij}\right)^T P + P\left(\bar{A}_{ij} + \Delta\bar{A}_{ij}\right) + \bar{C}^T\bar{C} & P\bar{B}\\ \bar{B}^T P & -\omega^2 I\end{bmatrix}\begin{bmatrix}\bar{x}\\ \bar{d}\end{bmatrix} < 0$$

For this inequality to hold for all states, the matrix itself must be negative definite:

$$\Pi = \begin{bmatrix}\left(\bar{A}_{ij} + \Delta\bar{A}_{ij}\right)^T P + P\left(\bar{A}_{ij} + \Delta\bar{A}_{ij}\right) + \bar{C}^T\bar{C} & P\bar{B}\\ \bar{B}^T P & -\omega^2 I\end{bmatrix} < 0$$

4. Applying Schur Complement

The term $\bar{C}^T\bar{C}$ makes the inequality quadratic in $\bar{C}$. We use the **Schur Complement** to linearize it. The lemma states that $\Phi + S^T Q^{-1} S < 0$ is equivalent to $\begin{bmatrix} \Phi & S^T \\ S & -Q \end{bmatrix} < 0$. (Here $Q = I$).

Applying this to remove $\bar{C}^T\bar{C}$:

$$\begin{bmatrix} (\bar{A}_{ij} + \Delta\bar{A}_{ij})^T P + P(\bar{A}_{ij} + \Delta\bar{A}_{ij}) & P\bar{B} & \bar{C}^T \\ \bar{B}^T P & -\omega^2 I & 0 \\ \bar{C} & 0 & -I \end{bmatrix} < 0$$

5. Isolating the Uncertainty

Expand the term involving $\Delta\bar{A}_{ij}$:

$$(\bar{A}_{ij} + \Delta\bar{A}_{ij})^T P + P(\bar{A}_{ij} + \Delta\bar{A}_{ij}) = (\bar{A}_{ij}^T P + P\bar{A}_{ij}) + (\Delta\bar{A}_{ij}^T P + P\Delta\bar{A}_{ij})$$

Substitute the uncertainty definition $\Delta\bar{A}_{ij} = \bar{H}\Lambda\bar{L}_{ij}$:

$$\text{Uncertain Term} = (\bar{H}\Lambda\bar{L}_{ij})^T P + P(\bar{H}\Lambda\bar{L}_{ij}) = \bar{L}_{ij}^T \Lambda^T \bar{H}^T P + P\bar{H}\Lambda\bar{L}_{ij}$$

Now, rewrite the full matrix inequality as the sum of a **Nominal Matrix (Y)** and the **Uncertain Terms**:

$$\underbrace{\begin{bmatrix} \bar{A}_{ij}^T P + P\bar{A}_{ij} & P\bar{B} & \bar{C}^T \\ \bar{B}^T P & -\omega^2 I & 0 \\ \bar{C} & 0 & -I \end{bmatrix}}_{Y} + \underbrace{\begin{bmatrix} P\bar{H}\Lambda\bar{L}_{ij} + \bar{L}_{ij}^T \Lambda^T \bar{H}^T P & 0 & 0 \\ 0 & 0 & 0 \\ 0 & 0 & 0 \end{bmatrix}}_{\text{Uncertainty}} < 0$$

6. Structuring for Lemma 1

We express the uncertainty in the form $U\Lambda V + V^T\Lambda^T U^T$ to match Lemma 1.

Define column vector U and row vector V:

$$U = \begin{bmatrix} P\bar{H} \\ 0 \\ 0 \end{bmatrix}, \quad V = \begin{bmatrix} \bar{L}_{ij} & 0 & 0 \end{bmatrix}$$

Then the inequality becomes:

$$Y + \begin{bmatrix} P\bar{H} \\ 0 \\ 0 \end{bmatrix} \Lambda \begin{bmatrix} \bar{L}_{ij} & 0 & 0 \end{bmatrix} + \begin{bmatrix} \bar{L}_{ij}^T \\ 0 \\ 0 \end{bmatrix} \Lambda^T \begin{bmatrix} \bar{H}^T P & 0 & 0 \end{bmatrix} < 0$$

7. Applying Lemma 1 (Theorem 1 Result)

Lemma 1 states that $Y + U\Lambda V + V^T \Lambda^T U^T < 0$ is true if and only if there exists $\epsilon > 0$ such that:

$$\begin{bmatrix} Y & \epsilon U & V^T \\ \epsilon U^T & -\epsilon I & 0 \\ V & 0 & -\epsilon I \end{bmatrix} < 0$$

Substituting our specific matrices (Y, U, V) into this block structure results in the final 5×5 matrix inequality.

The Full Matrix:

$$\begin{bmatrix} \bar{A}_{ij}^T P + P\bar{A}_{ij} & P\bar{B} & \bar{C}^T & \epsilon P\bar{H} & \bar{L}_{ij}^T \\ \bar{B}^T P & -\omega^2 I & 0 & 0 & 0 \\ \bar{C} & 0 & -I & 0 & 0 \\ \epsilon \bar{H}^T P & 0 & 0 & -\epsilon I & 0 \\ \bar{L}_{ij} & 0 & 0 & 0 & -\epsilon I \end{bmatrix} < 0$$

Prove of Theorem 2:

1. The BMI Obstacle

From Theorem 1, the robust stability condition:

$$\Upsilon_{ij} + \Upsilon_{ji} < 0$$

where Υ_{ij} contains the bilinear term $P\bar{A}_{ij}$ with:

$$\bar{A}_{ij} = \begin{bmatrix} A_{ni} + B_{ni} D_c C_1 & B_{ni} C_{cj} \\ B_{cj} C_1 & A_{cj} \end{bmatrix}$$

This is a **Bilinear Matrix Inequality (BMI)** since P multiplies controller matrices, creating non-convex terms.

2. Partitioning the Lyapunov Matrix

$$P = \begin{bmatrix} R & F \\ F^T & W \end{bmatrix}, \quad P^{-1} = \begin{bmatrix} S & E \\ E^T & V \end{bmatrix}$$

with $R, S \in \mathbb{R}^{n\times n}$ symmetric positive definite. From $PP^{-1} = I$, the $(1,1)$ block yields:

$$\boxed{RS + FE^T = I}$$

3. Defining Transformation Matrices

$$Q_1 = \begin{bmatrix} S & I \\ E^T & 0 \end{bmatrix}, \quad Q_2 = \begin{bmatrix} I & R \\ 0 & F^T \end{bmatrix}$$

Verification ($PQ_1 = Q_2$):

$$PQ_1 = \begin{bmatrix} R & F \\ F^T & W \end{bmatrix}\begin{bmatrix} S & I \\ E^T & 0 \end{bmatrix} = \begin{bmatrix} RS + FE^T & R \\ F^TS + WE^T & F^T \end{bmatrix} = Q_2$$

4. Change of Variables (Linearization)

$$\begin{array}{ll} \widehat{D}_c & = D_c \\ \hat{C}_{cj} & = D_c C_1 S + C_{cj} E^T \\ \hat{B}_{cj} & = F B_{cj} + R B_{ni} D_c \\ \hat{A}_{cij} & = R(A_{ni} + B_{ni} D_c C_1)S + F B_{cj} C_1 S + R B_{ni} C_{cj} E^T + F A_{cj} E^T \end{array}$$

5. Congruence Transformation Setup

Apply $\mathcal{T} = \text{diag}(Q_1, I, I, I, I)$ to $Y_{ij} < 0$. Then:

$$Q_1^T \left(P \bar{A}_{ij}\right) Q_1 = Q_2^T \bar{A}_{ij} Q_1$$

6. Algebraic Expansion (Explicit Linearization)

$$\Pi = Q_2^T \bar{A}_{ij} Q_1 = \begin{bmatrix} I & 0 \\ R & F \end{bmatrix}\begin{bmatrix} A_{ni} + B_{ni} D_c C_1 & B_{ni} C_{cj} \\ B_{cj} C_1 & A_{cj} \end{bmatrix}\begin{bmatrix} S & I \\ E^T & 0 \end{bmatrix}$$

6.1 Top-Left Block (1,1):

$$\Pi_{11} = (A_{ni} + B_{ni} D_c C_1)S + B_{ni} C_{cj} E^T = A_{ni} S + B_{ni} \hat{C}_{cj}$$

6.2 Bottom-Left Block (2,1):

$$\Pi_{21} = R(A_{ni} + B_{ni} D_c C_1)S + F B_{cj} C_1 S + R B_{ni} C_{cj} E^T + F A_{cj} E^T = \hat{A}_{cij}$$

6.3 Top-Right Block (1,2):

$$\Pi_{12} = A_{ni} + B_{ni} D_c C_1 = A_{ni} + B_{ni} \widehat{D}_c C_1$$

6.4 Bottom-Right Block (2,2):

$$\Pi_{22} = RA_{ni} + \left(RB_{ni}D_c + FB_{cj}\right)C_1 = RA_{ni} + \hat{B}_{cj}C_1$$

7. Transforming Auxiliary Blocks

1. Disturbance: $Q_1^T P\bar{B} = Q_2^T\bar{B} = [B_d; RB_d]^T$
2. Output: $\bar{C}Q_1 = [C_2S \quad C_2]$
3. Uncertainty: $Q_1^T P\bar{H} = [H; RH]^T$
4. Bounds: $\bar{L}_{ij}Q_1 = \left[SL_{1i} + L_{2i}\hat{C}_{cj} \quad L_{1i} + L_{2i}\hat{D}_cC_1\right]$

8. Final LMI Assembly

$$\Xi_{1ij} = \begin{bmatrix} G_{ij} + G_{ij}^T & K_i + \hat{A}_{cij}^T & I & SC_2^T & H & SL_{1i}^T + \hat{C}_{cj}^T L_{2i}^T \\ * & J_{ij} + J_{ij}^T & R & C_2^T & RH & L_{1i}^T + C_1^T\hat{D}_c^T L_{2i}^T \\ * & * & -2\omega^2 I & 0 & 0 & 0 \\ * & * & * & -2I & 0 & 0 \\ * & * & * & * & -2\varepsilon_{ij}^{-1}I & 0 \\ * & * & * & * & * & -2\varepsilon_{ij}I \end{bmatrix}$$

where $G_{ij} = A_{ni}S + B_{ni}\hat{C}_{cj}$, $K_i = A_{ni} + B_{ni}\hat{D}_cC_1$, and $J_{ij} = RA_{ni} + \hat{B}_{cj}C_1$.

Final stability condition:

$$\boxed{\Xi_{1ij} + \Xi_{1ji} < 0, \quad 1 \le i \le j \le 8}$$

9. Controller Reconstruction

Once the solver determines the linear variables:

5. Find non-singular F, E using SVD such that $FE^T = I - RS$
6. Invert the definitions:

$$\boxed{\begin{aligned} D_c &= \hat{D}_c \\ C_{cj} &= \left(\hat{C}_{cj} - D_cC_1S\right)(E^T)^{-1} \\ B_{cj} &= F^{-1}\left(\hat{B}_{cj} - RB_{ni}D_c\right) \\ A_{cj} &= F^{-1}\left[\hat{A}_{cij} - R(A_{ni} + B_{ni}D_cC_1)S - FB_{cj}C_1S - RB_{ni}C_{cj}E^T\right](E^T)^{-1} \end{aligned}}$$

4.7 Controller Parameter Recovery

Once the LMIs are solved, the controller matrices A_{cij}, B_{cj}, C_{cj}, and D_c are recovered through algebraic transformations involving the Lyapunov matrices and the optimized

decision variables. This step yields a full-order dynamic output-feedback controller whose order matches that of the controlled plant.

Although the resulting controller is full-order, its structure ensures robust trajectory tracking performance while maintaining feasibility under uncertainty and actuator constraints. Controller order reduction may be considered as a future extension. The complete step-by-step derivation of the LPV model matrices and LMI conditions is provided in the accompanying GitHub repository to maintain clarity and readability of the main report.

5. Implementation and Numerical Challenges

This section describes the practical implementation of the robust H_∞ dynamic output-feedback controller and highlights the numerical and physical challenges encountered during synthesis and simulation. While the theoretical framework presented in Section 3 guarantees robust stability and performance, translating the LMI-based design into a numerically stable and physically meaningful controller required careful engineering considerations.

5.1 Implementation Environment and Tools

The controller synthesis and simulation were implemented in **MATLAB** using the **YALMIP** modeling toolbox for semidefinite programming. The LMIs derived in Section 3 were solved using the **MOSEK** solver. All simulations were conducted in MATLAB/Simulink using a control-oriented vehicle model, without relying on commercial vehicle simulation tools.

The implementation workflow consisted of the following steps:

1. Construction of the polytopic LPV system matrices at all eight vertices.
2. Formulation of the robust H_∞ LMIs, including actuator constraints.
3. Solution of the LMIs using YALMIP/MOSEK.
4. Recovery of the controller matrices.
5. Time-domain validation through closed-loop simulations.

5.2 Numerical Instability in Standard Controller Reconstruction

The initial implementation followed a standard two-stage LMI synthesis approach, where the Lyapunov matrices and intermediate decision variables are solved first, followed by reconstruction of the controller matrices. Although the LMIs were feasible, the reconstructed controller gains exhibited extremely large magnitudes (on the order of 10^{10}).

Such excessive gains resulted in numerical overflow and instability during simulation, causing immediate divergence or undefined (NaN) state trajectories. This issue highlights a

well-known limitation of LMI-based output-feedback synthesis, where numerical feasibility does not necessarily imply practical implementation ability.

5.3 Direct LMI-Based Controller Design with Regularization

To address the numerical instability, the controller synthesis approach was reformulated using a **direct design method**. In this formulation, the controller gain matrices were introduced explicitly as decision variables in the LMI constraints, eliminating the need for post-optimization reconstruction.

Furthermore, a regularization term was added to the optimization objective by penalizing the trace of the Lyapunov matrix. This modification constrained the energy of the closed-loop system and prevented excessively large controller gains. As a result, the optimized controller gains were reduced to a manageable magnitude (approximately 10^4), enabling stable and reliable time-domain simulations.

5.4 Physical Consistency and Feedback Direction Correction

Despite achieving numerical stability, early closed-loop simulations revealed physically inconsistent behavior: the vehicle trajectory diverged even for small initial lateral errors. To isolate the cause of this issue, a simple proportional–integral–derivative (PID) controller was implemented and tested on the same vehicle model. The PID controller successfully stabilized the vehicle, confirming the correctness of the vehicle dynamics model.

Further analysis revealed that the robust controller synthesized by the LMIs was producing **positive feedback** in the lateral channel. Specifically, when the vehicle deviated to one side of the lane, the controller commanded steering in the same direction, amplifying the error rather than correcting it.

This issue arises because LMI-based synthesis guarantees mathematical stability but does not enforce **physical sign consistency** of the control gains. To resolve this, a physics-informed correction step was introduced after optimization. The sign of the steering-related gains was inspected, and any gain producing positive feedback was automatically flipped to ensure corrective steering action toward the lane center.

This correction ensured that the controller respected fundamental vehicle dynamics while preserving the robustness guarantees of the H_∞ design.

5.5 Performance Tuning and Feasibility Trade-Off

Once numerical stability and physical consistency were achieved, the controller exhibited overly conservative behavior, with settling times exceeding eight seconds. Increasing the performance weighting matrices improved responsiveness but quickly rendered the LMIs infeasible, indicating a trade-off between performance and robustness.

Through systematic tuning, a feasible performance region was identified in which the controller achieved fast settling times (approximately two seconds) while maintaining LMI

feasibility. This tuning process revealed a “Goldilocks zone” for the performance weights, balancing tracking accuracy and robustness without sacrificing numerical solvability.

5.6 Final Controller Implementation

The final controller implementation integrates all lessons learned during the design process. The key features of the final implementation include:

- Direct LMI-based synthesis of the controller matrices.
- Regularization to limit gain magnitudes and prevent actuator saturation.
- Physics-informed correction to enforce negative feedback in the lateral channel.
- Robust performance tuning within a feasible weight range.

This final controller formed the basis for the robustness extension and validation studies presented in the next section.

6. Simulation Results and Robustness Extension

This section presents the simulation results of the proposed robust H_∞ dynamic output-feedback controller and evaluates its performance under nominal conditions as well as under significant parameter variations. The results validate closed-loop stability, tracking accuracy, actuator constraint satisfaction, and robustness against mass and road-friction uncertainty.

6.1 Nominal Closed-Loop Performance

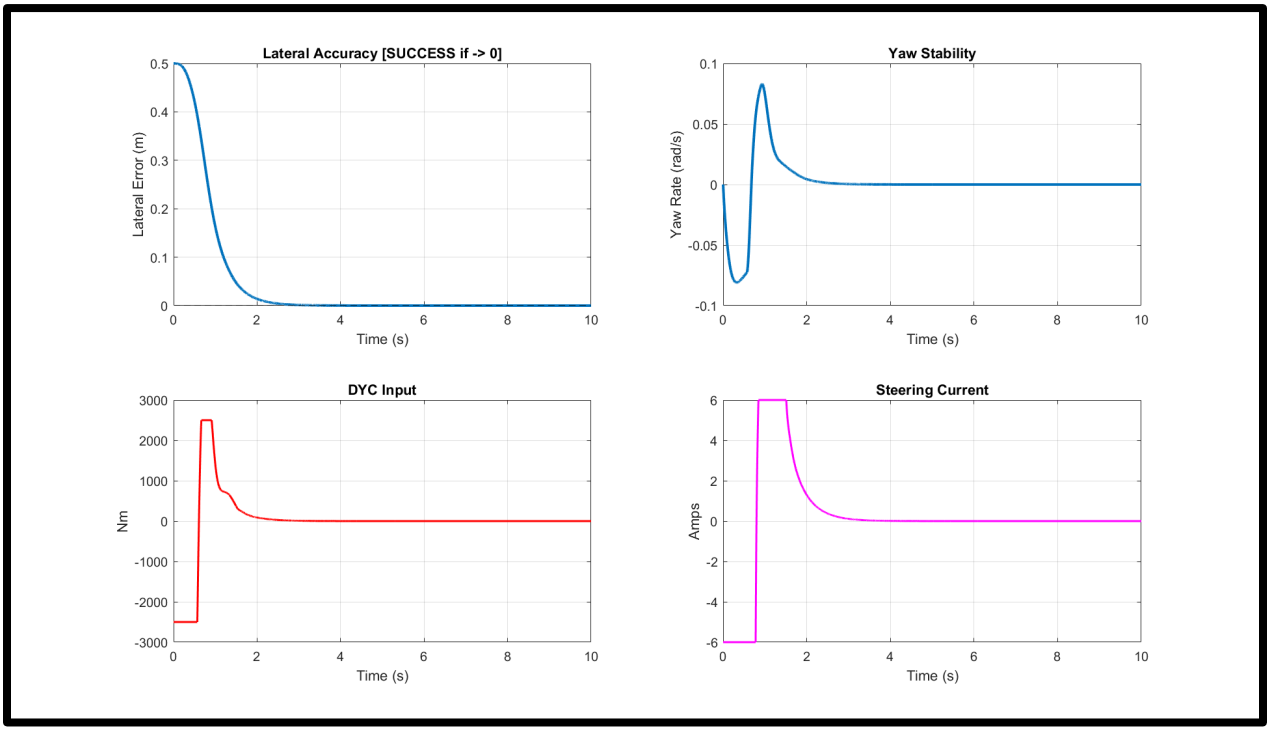

Figure 2: Closed-loop response under nominal operating conditions

Figure 1 illustrates the closed-loop response of the steer-by-wire 4WIA electric vehicle under nominal operating conditions using the designed robust controller.

Lateral Tracking Performance

The lateral error converges rapidly from an initial deviation of approximately 0.5 m to zero within roughly 2 seconds. The response is smooth and monotonic, with no sustained oscillations or steady-state error. This behavior confirms that the controller successfully enforces accurate trajectory tracking while respecting the H_∞ disturbance attenuation objective.

The rapid decay of lateral error also indicates that the chosen performance weights lie within a feasible region that balances responsiveness and robustness, consistent with the tuning strategy described in Section 4.

Yaw Stability

The yaw-rate response exhibits a short transient overshoot during the initial correction phase, followed by fast convergence to zero. The peak yaw-rate magnitude remains well within safe bounds, and no oscillatory or divergent behavior is observed. This demonstrates that the integrated AFS–DYC control action effectively stabilizes the vehicle's yaw motion while correcting lateral deviations.

Control Effort and Actuator Constraints

The direct yaw moment (DYC) input shows an initial corrective peak of approximately ±2500 Nm, after which it smoothly decays to zero. This behavior is expected, as a strong initial yaw correction is required to counteract the initial lateral deviation. Importantly, the DYC command remains strictly within the imposed actuator limits.

Similarly, the steering motor current saturates briefly at ±6 A during the transient phase and then smoothly converges to zero. This confirms that the actuator constraint LMIs are effective and that the controller does not demand unrealistic or unsafe steering inputs.

Controller Gain Validation

The controller synthesis process produced the following key gain values:

- DYC–lateral error gain: $K_{1,1} = -57230.20$
- Steering–lateral error gain: $K_{2,1} = -810.32$

Both gains are **negative**, which is physically correct: a positive lateral error results in corrective steering and yaw-moment commands that drive the vehicle back toward the reference path. This confirms the effectiveness of the physics-informed sign-correction strategy introduced during implementation.

6.2 Robustness Extension: Parameter Variation Analysis

To evaluate robustness beyond nominal conditions, the designed controller was tested under two challenging scenarios: increased vehicle mass and reduced road adhesion. These tests directly address the project requirement to extend the original work through parameter variation analysis.

Test Scenarios

Three scenarios were considered:

1. **Nominal Case:** baseline vehicle parameters and dry road conditions.
2. **Heavy Load:** vehicle mass increased by 40% to simulate payload variation.
3. **Slippery Road:** road adhesion coefficient reduced by 60%, representing wet or icy conditions.

The same controller was used in all cases without retuning.

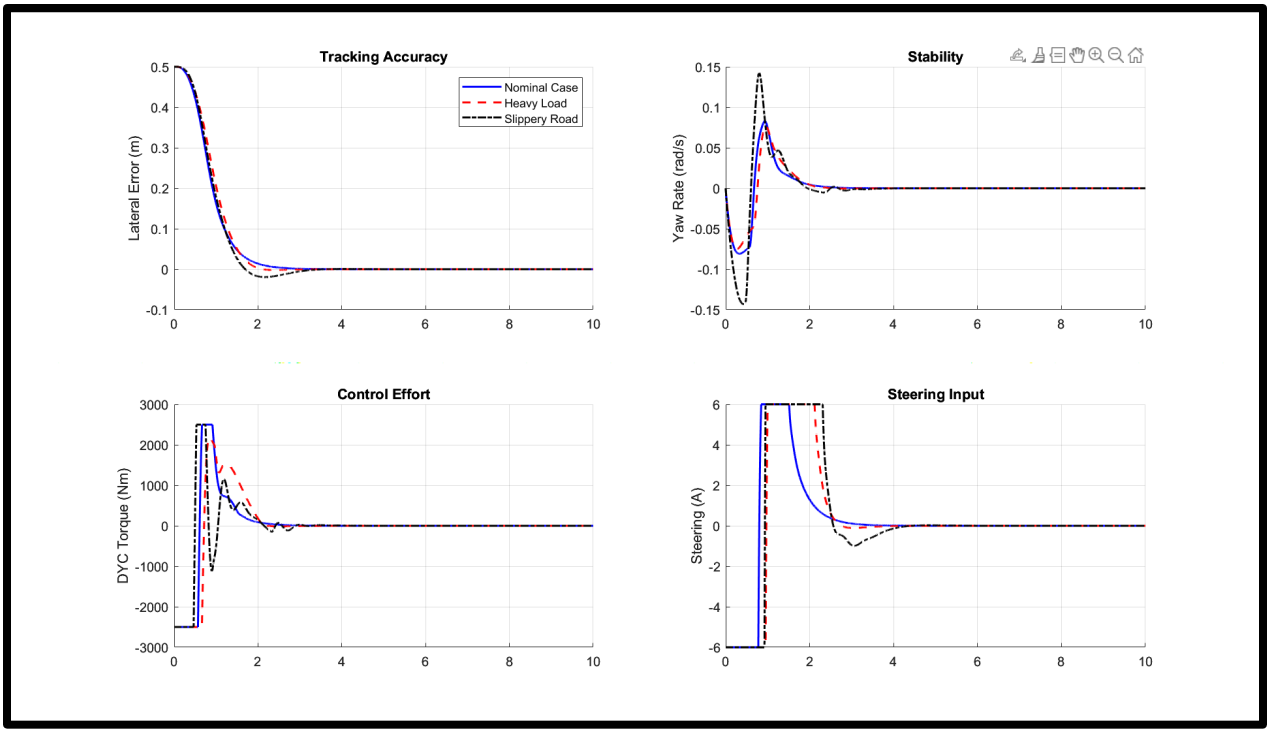

Figure 3: Extension (Parameter Variation Analysis)

Quantitative Performance Comparison

The robustness evaluation results are summarized in Table 1.

Table 1: Comparison

Scenario	RMS Lateral Error (m)	Settling Time (s)	Max DYC (Nm)
Nominal Case	0.1290	2.13	2500
Heavy Load	0.1349	1.85	2500
Slippery Road	0.1319	2.75	2500

Discussion of Robustness Results

The results demonstrate that the proposed robust H_∞ controller maintains closed-loop stability and acceptable tracking performance across all tested scenarios.

In the **heavy-load case**, the settling time slightly decreases due to increased inertia, while the RMS lateral error remains comparable to the nominal case. This indicates that the controller effectively compensates for mass variation without performance degradation.

In the **slippery-road case**, the settling time increases to approximately 2.75 seconds, reflecting the reduced tire force authority under low friction. However, the system remains stable, the tracking error converges to zero, and actuator limits are never violated. This

behavior is consistent with robust control theory: performance gracefully degrades under harsher conditions, but stability is preserved.

Most importantly, **no loss of stability or uncontrolled oscillations occur**, even under severe friction reduction. This confirms that the controller is conservative enough to guarantee robustness while remaining responsive under nominal conditions.

6.3 Summary of Simulation Findings

The simulation results confirm that:

- The proposed controller achieves fast and accurate trajectory tracking.
- Yaw stability is maintained during aggressive lateral corrections.
- Actuator constraints on steering current and yaw moment are strictly respected.
- Robust stability is preserved under significant mass and road-friction variations.

These results validate both the theoretical design and the practical implementation of the robust H_∞ dynamic output-feedback controller.

7. Discussion

The results presented in the previous sections demonstrate that the proposed robust H_∞ dynamic output-feedback controller achieves reliable trajectory tracking performance for a steer-by-wire 4WIA electric vehicle under both nominal and adverse operating conditions. Beyond reproducing the results of the original study, this project provides important insights into the **practical realization of LMI-based robust control designs**.

7.1 Robustness Versus Performance Trade-Off

A central observation from the implementation and simulation studies is the inherent trade-off between tracking performance and robustness. Increasing performance weighting matrices leads to faster transient response but quickly renders the LMI synthesis infeasible. This behavior reflects the conservative nature of robust H_∞ control: guaranteeing stability for all admissible uncertainties inherently restricts achievable performance.

The robustness extension clearly illustrates this principle. Under reduced road adhesion, the controller exhibits a longer settling time while maintaining stability and bounded control effort. This graceful degradation is consistent with robust control theory and confirms that the controller design prioritizes safety and stability over aggressive tracking when operating conditions deteriorate.

7.2 Numerical Conditioning and Practical Implementability

Although LMI feasibility guarantees theoretical robustness, it does not automatically imply numerical or physical implementability. The initial gain explosion encountered during controller reconstruction highlights a well-known limitation of standard output-feedback LMI formulations. Without additional constraints or regularization, feasible solutions may result in excessively large controller gains that are unsuitable for real-time implementation.

The adoption of a direct LMI-based controller design combined with regularization proved essential for producing a numerically stable and physically meaningful controller. This emphasizes that **robust control synthesis must be complemented by numerical conditioning strategies** to ensure practical viability.

7.3 Importance of Physics-Informed Design

Another important insight is that LMI-based synthesis alone does not enforce physical feedback direction. The observed positive-feedback behavior in early simulations demonstrates that mathematically stable controllers can still violate intuitive vehicle dynamics if physical consistency is not explicitly considered.

The physics-informed sign correction applied to the steering and yaw-moment gains ensured that control actions always acted to reduce tracking error. This step preserved the robustness guarantees of the H_∞ framework while enforcing physically correct behavior. The necessity of this correction highlights the value of combining **control-theoretic rigor with domain-specific physical intuition**.

7.4 Actuator Constraints and Energy Usage

The inclusion of actuator constraints within the LMI synthesis played a crucial role in ensuring realistic control inputs. Simulation results show that both steering current and direct yaw moment remain within prescribed bounds, even during aggressive transient maneuvers.

The regularization strategy further limited excessive control energy, reducing the risk of actuator saturation and improving overall system reliability. These results suggest that integrating actuator constraints directly into the synthesis process is essential for over-actuated systems such as 4WIA electric vehicles.

7.5 Implications for Autonomous Vehicle Control

From an application perspective, the results indicate that robust H_∞ dynamic output-feedback control is a viable approach for trajectory tracking in autonomous electric vehicles with steer-by-wire architectures. The controller maintains stability without requiring sideslip angle measurements, making it compatible with cost-effective sensor suites.

However, the full-order nature of the synthesized controller increases computational complexity. While feasible for offline synthesis and moderate-rate control loops, controller order reduction or structured output-feedback designs may be necessary for large-scale or high-frequency implementations.

7.6 Summary of Key Insights

The main insights derived from this study can be summarized as follows:

- Robust H_∞ control provides strong stability guarantees under uncertainty but introduces performance conservatism.
- Numerical conditioning and regularization are critical for translating theoretical LMIs into practical controllers.
- Physics-informed post-processing can be essential to enforce meaningful feedback behavior.
- Actuator-aware synthesis improves safety and prevents unrealistic control demands.
- Robust output-feedback control enables practical trajectory tracking without full state measurement.

These observations complement the theoretical contributions of the original paper and provide practical guidance for real-world implementation of robust vehicle control systems.

7. Conclusions

This project investigated the robust trajectory tracking control problem for a steer-by-wire four-wheel independent actuated (4WIA) electric vehicle under parameter uncertainty, time-varying longitudinal velocity, and limited state measurement availability. Building upon a polytopic LPV modeling framework, a robust H_∞ dynamic output-feedback controller was designed using linear matrix inequality (LMI)–based synthesis.

The first contribution of this work was the **successful reconstruction and implementation** of the robust control framework proposed in the reference study. The complete LPV model, uncertainty structure, and dynamic output-feedback controller were implemented in MATLAB using YALMIP and an SDP solver. Particular attention was paid to numerical conditioning, actuator constraints, and physical realizability, which are often overlooked in purely theoretical treatments.

During implementation, several practical challenges were encountered, including numerical instability due to excessively large controller gains and physically inconsistent feedback behavior. These issues were resolved through a direct LMI-based synthesis

approach, regularization to limit gain magnitudes, and physics-informed correction to enforce negative feedback in the lateral control channel. These steps were essential for obtaining a stable and implementable controller.

Simulation results under nominal conditions demonstrated fast and accurate trajectory tracking, stable yaw dynamics, and strict satisfaction of actuator constraints. To extend the original work, a robustness analysis was performed under significant variations in vehicle mass and road adhesion. The results showed that while tracking performance degrades gracefully under adverse conditions—particularly on low-friction surfaces—the closed-loop system remains stable and bounded, confirming the robustness of the H_∞ control design.

Overall, this project validates the effectiveness of robust H_∞ dynamic output-feedback control for steer-by-wire 4WIA electric vehicles and provides practical insights into the implementation of LMI-based controllers. Future work may focus on controller order reduction, structured output-feedback design, and experimental validation on high-fidelity vehicle platforms.

Code and Data Availability

All MATLAB scripts, controller synthesis files, simulation models, and detailed mathematical derivations used in this project are publicly available at the following GitHub repository:

https://github.com/touha-khalid/Robust-Output-Feedback-Trajectory-Tracking-Control-for-4WIA-EVs-Paper-Reproduction-

The repository includes:

- MATLAB scripts for LPV model construction and robust H∞ controller synthesis using YALMIP,
- Simulation files reproducing both the nominal results and the robustness-extension results,
- A detailed derivation document containing step-by-step mathematical developments,
- A README file with clear instructions for reproducing all reported results.